J. S. Afr. Inst. Min. Metall., vol. 86, no. 2.
Feb. 1986. pp. 51-60.

Response of mine hoisting cables to longitudinal shock loads

by R.R. MANKOWSKI* and F.J. COX†

SYNOPSIS

Experimental results are presented on the longitudinal attenuation of a kinetic shock wave travelling along a typical mine hoisting cable. Mathematical curve-fitting of the results established these losses to be exponential and tension-dependent.

The reflection and power-transmission coefficients of a typical winding drum were also investigated. The degree of penetration of an incident stress wave onto the coil of cable wrapped round the drum is shown to be governed by a second-degree relationship, and is solely dependent on the acceleration of the cable at the cable–drum interface.

Although the investigation is limited to the testing of a single hoisting cable, certain qualitative trends that were identified can be generalized and applied to other types of hoisting cable with different geometries, elastic properties, and installations.

SAMEVATTING

Die resultate van eksperimente in verband met die oorlangse verswakking van 'n kinetiese skokgolf wat langs 'n tipiese mynhyskabel beweeg, word aangegee. Wiskundige krommepassing van die resultate het vasgestel dat hierdie verliese eksponensiaal en van die spanning afhanklik is.

Die refleksie- en kragoorbringingskoëffisiënt van 'n tipiese hystrommel is ook ondersoek. Daar word getoon dat die mate van indrywing van 'n invallende spanningsgolf op die rol kabel wat om die trommel gewikkel is, deur 'n tweedegraadse verhouding beheer word en uitsluitlik van die versnelling van die kabel by die vlak tussen die kabel en die trommel afhang.

Hoewel die ondersoek beperk word tot die toets van 'n enkelhyskabel, kan sekere kwalitatiewe tendense wat geïdentifiseer is, veralgemeen word en op ander soorte hyskabels met ander geometrieë, elastiese eienskappe en installasies toegepas word.

Introduction

A century ago, the depth of mining shafts never exceeded a few hundred metres, and the hoisting speeds of the cables used in lifting the ore were not considered to be mechanically detrimental. As mining has progressed to greater depths, the need to make optimum use of the shafts has led to increased winding depths, speeds, and payloads.

In the past few decades, mining engineers have had to take serious cognizance of the undesirable effects associated with the extraction of ore from thousands of metres underground at hoisting speeds of up to 18 $m \cdot s^{-1}$. Mine engineers met the challenge by developing multi-cable systems each having certain advantages in the light of local conditions, and manufacturers of mining cables contributed by developing improved high-strength wires with a variety of sections and lays to meet specific conditions.

In spite of sustained efforts by mining engineers to improve existing methods for the achievement of safe, efficient mining operations and the reduction of cable fatigue to an absolute minimum, the dynamic behaviour of hoisting cables has always caused concern. These cables are subject to vibrations that cannot be suppressed completely, and that raise the level of dynamic stress and friction wear while reducing the safe life of the cables. Under extreme conditions, the safety of men and plant can be at risk.

* Senior Lecturer, Department of Mechanical Engineering.
† Senior Lecturer, Department of Electrical Engineering.
Both of the University of Durban-Westville, Private Bag X54001, Durban 4000.

SA ISSN 0038-223X/$3.00 + 0.00. Paper received 25th May, 1985.

The general problem of vibrations in mine cables has been aptly stated in the work of Dimitriou and Whillier[1] and Jordan[2], who suggest that an analysis should be based on the formulation and solution of non-linear differential equations. Implicit in their discussion is the belief that, owing to the restrictive assumptions and approximations made in the derivation of differential equations, qualitative results obtained through such a process do not necessarily reflect the true nature of the phenomena. In an alternative approach, the overall behaviour of such systems is considered to be the cumulative result of isolated phenomena acting concurrently. However, such a cumulative analysis depends strongly on the additive nature of the individual phenomena, which could lead to errors, especially if the behaviour is non-linear.

Exact solutions to non-linear hyperbolic systems are few and limited to very special cases. Mathematicians have developed a variety of procedures for their approximate solution, but these procedures are complicated and tedious, even for relatively simple vibrating systems. However, progress has been made and continues to be made in the development of non-linear concepts that have general applicability.

In attempting to achieve formalized solutions of highly non-linear problems, some researchers adopt restrictive assumptions, which tend to constrain the analysis into a seemingly intractable system of equations. While these attempts produce valid results and break fresh ground for future research, it is felt that a strict mathematical approach sometimes fails to clarify the true physical nature of the phenomena. In the study of hyperbolic systems in particular, this failure generally manifests itself in the form of an assumed solution that neglects the fun-

damental mechanical cause of the motion. As propagating stress waves are the basic cause of cable motion in most practical situations, an understanding of the speeds at which they propagate, the associated attenuation, and the fundamental laws of wave mechanics that they obey is essential. This motivated the experimental investigation described here, which sets out to quantify some of the dynamic properties associated with the transmission, reflection, and attenuation of longitudinal stress waves occurring at the interface between the cable and the winding drum in a typical single-drum winding system. The penetration and attenuation of stress waves around the winding drum were also investigated.

The symbols used are defined at the end of the paper.

Experimental Apparatus

A full-scale winding-drum section in the form of a cylinder was constructed in the Structures Laboratory of the Faculty of Engineering at the University of Durban-Westville (Fig. 1). The height of the cylinder is 300 mm and the diameter 4260 mm. A circular mild-steel sheet 10 mm thick was used to line the surface of the cylinder, and rigidity of the structure was achieved by the installation of sufficient reinforcing bar, shear cages, and steel mesh, and the filling of the cylinder with concrete of 40 MPa strength.

Rectangular steel cleats welded to the inside of the liner ensure that there is no slippage of the liner relative to the concrete. Fifteen bolts of 50 mm diameter passing through the concrete floor are tensioned to secure the section to the floor. The effective mass movement of inertia of the cylinder can be assumed to be infinite because (for all practical purposes) the rotation and translation of the cylinder relative to the floor are eliminated.

Two individual lengths of cable comprise the first and second layer, and both are 43,5 mm (nominal diameter) with construction 6 × 32 (14/12/6 tri)/F, actual breaking load of 1406 kN, and linear mass density of 7,33 $kg \cdot m^{-1}$. The first layer of cable is wrapped helically round the drum section and restrained vertically by spaced angle-iron sections welded onto the liner. The four coils of cable making up the first layer were pretensioned to 40 kN before being fastened to stay posts near the drum section. The second layer consists of three coils wrapped in the helical grooves formed by the first layer. One end of the second layer is fastened to a nearby stay post, while the other end, fitted with a white-metal conical socket, is stretched horizontally across the floor and fitted into a hydraulic tensioning device. The tensioning device (Fig. 2) is also capable of exciting the conical socket with a purely longitudinal impact load in the direction of increasing tension.

The longitudinal impact is achieved by a falling mass attached to a pendulum arm. The impact mass is constructed in the shape of an inverted U to ensure no interference with the cable and to make it possible for the centre of gravity of the impact mass to be aligned with the longitudinal centroid of the cable. During operation, the pendulum arm is raised to the horizontal position, and is released by a mechanical trigger. To obviate the risk of misalignment between the impact mass and the impact collar during collision, the impact mass was given three degrees of freedom. For an arbitrary fixed cable tension, the impact mass could then be aligned manually and locked into position for positive contact with the impact collar prior to impact.

The impact velocity and the magnitude of the subsequent dynamic stress wave imparted to the cable are determined from the energy balance and linear momentum equations.

Pre-tensioning of the cable was achieved by two symetrically placed 500 kN hydraulic jacks acting against the cross-head. Cable creep around the drum section was compensated for by adjustment of the two slack nuts behind the cross-head.

An accelerometer is used to monitor the intensities and arrival times of wave fronts propagating along the cable. The accelerometer is mounted on a special block under which a helical knife-edge is welded. When clamped into position, the helical knife-edge mates with the lay angle of the cable strand, and the direction of primary sensitivity of the accelerometer is parallel to the longitudinal axis of the cable. The output of the accelerometer is first passed through a charge amplifier, and the signal is then fed through a low-pass filter (with a cut-off frequency that is variable over the range 100 to 500 Hz), and is finally stored digitally on disc in a Nicolette digital storage oscilloscope (D.S.O.) for further processing.

An amplified signal coming from an identical accelerometer mounted on the housing of the white-metal socket is used to excite the external-trigger mode of the D.S.O. Thus, all the wave events for each individual test are referenced to the instant of impact.

Experimental Procedure

The attenuation profile of a single impact pulse was obtained as follows. The accelerometer probe was moved along the length of free cable and then onto clamps pre-positioned on the second layer of cable on the drum section. When the probe was moved in increments of 1 m, as many as 20 station readings were required for the capture of a complete profile. As one profile is the result of 20 impact loadings at most, considerable care had to be taken to ensure that the pre-tension and impact energy were consistently of the same magnitude.

Tension in the free cable is monitored by a pressure gauge mounted in the hydraulic line pressurizing the jacks. The resolution of the pressure gauge is 0,05 MPa, which corresponds to an accuracy of 235 N in the desired tension.

Some interesting phenomena were observed during the initial stages of the experiment, particularly the relative motion between the second and the first layer. A change in the tension to either a higher or a lower value introduced a first-order effect in the tension after the change had taken place. Following an increase in tension (for example, that caused by a positive displacement of the cross-head over a time interval of 30 seconds), the average strain energy in the free cable was initially higher than the average strain energy in the second layer of cable. Owing to the mechanics of a 'bollard' type of friction, this difference resulted in an advance of a higher strain gradient round the coil of cable formed by the second layer. Once static equilibrium had been reached at the interface between the cable and the drum, the total strain energy in the second layer was increased while the strain energy

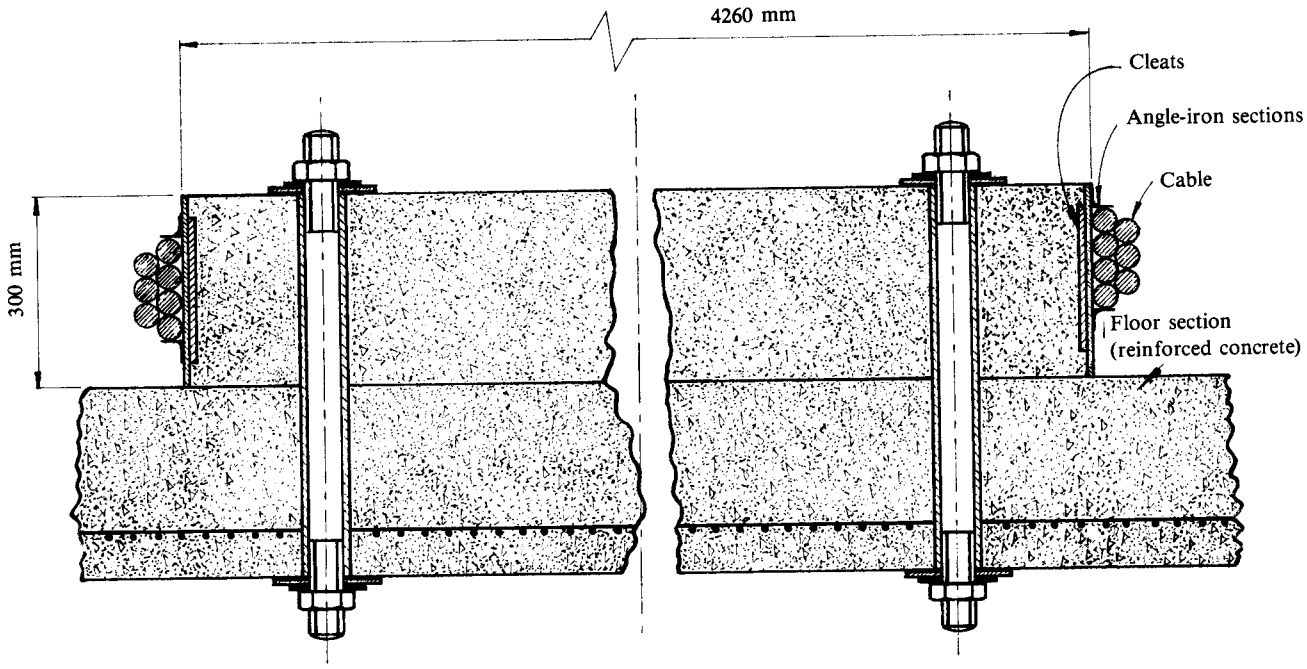

Fig. 1—Winding-drum section

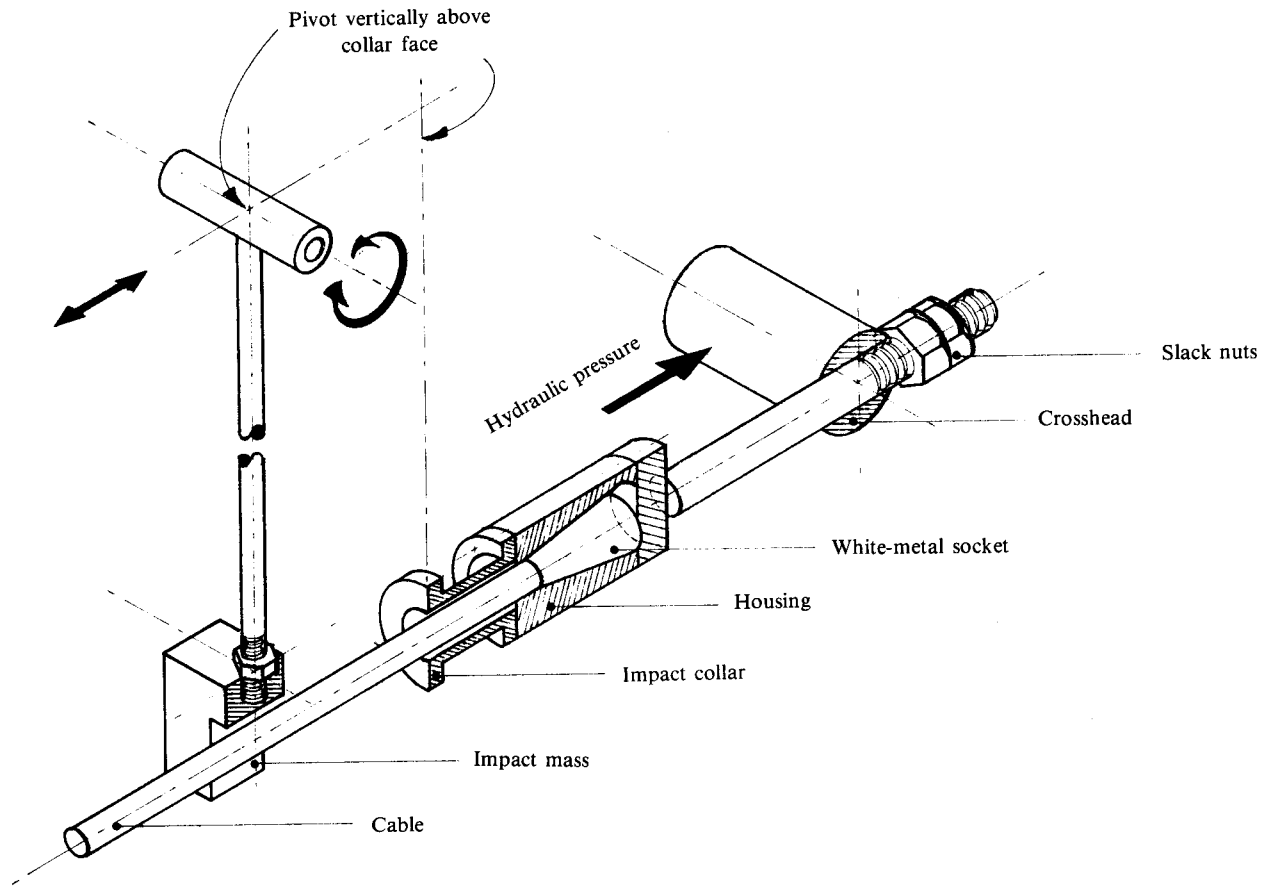

Fig. 2—Half-sectional isometric sketch showing the impact mass and tensioning mechanism

in the free cable was consequently reduced. This exchange or transfer of strain energy had the final effect of reducing the tension in the free cable.

Similarly, after a decrease in tension caused by an appropriate movement of the cross-head, the entrained strain energy in the second layer was slowly released into the free cable, causing the tension there to rise. While these effects are indeed second-order and the result of a series of high-frequency transmitted and reflected strain waves, the overall effect over a period of 3 to 5 minutes of settling can be generally termed a quasi-static first-order response.

This problem of settling was overcome when the position of the cross-head was fixed and the cable was then excited with a series of longitudinal impact loads via the impact mass. When no noticeable change in the free-cable tension had occurred after impact, the same impact mass and 'settled' cable tension were recorded and used to give a single profile. Experience gained in this manner made it a relatively easy task to set the free-cable tension to any prescribed value.

The time 'window' over which events were recorded on the D.S.O. was determined by the physical parameters of the system. A stress wave originating at the impact end travels the length of free cable and then penetrates the second layer. At the interface between the cable and the drum, theory predicts that a partially transmitted stress wave and a partially reflected stress wave should be in evidence. Over the limited range of cable tension and impact-loading magnitudes, the penetration of the transmitted stress wave was found not to exceed 9 m along the second layer measured circumferentially from the interface.

Preliminary experimental investigation determined the speed of propagation of a longitudinal pulse to be 4000 m/s. Given that the length of free cable was 13 m and the maximum penetration depth of the pulse on the drum section was 9 m, the largest fundamental period of a pulse was 11 ms. The assumption is therefore justified that, if there is evidence of a reflected wave in the free cable, its effects must necessarily be recorded in the interval 0 to 11 ms. For the purposes of this investigation, a scan rate of 10 ms was found to be the most suitable.

Results

Initially and for convenience, the vibration in the free cable and in the drum cable are considered separately. At a later stage, when the transmission of energy is investigated, the dynamic conditions at the interface will be treated as piecewise continuous.

Vibration of the Free Cable

The experimental variables used to give the attenuation profile of the free cable are tension and impact mass. For a fixed tension, three different impact masses were used to excite the cable: 24 kg, 29 kg, and 37 kg. The tension in turn was varied from 87,7 to 175,4 kN in increments of 17,5 kN. The three stations used repeatedly for the monitoring of acceleration in the free cable were stations 3, 6, and 9 as indicated in Fig. 3(b), the number assigned to a station being the distance in metres measured from a reference point set at 1,5 m from the impact end.

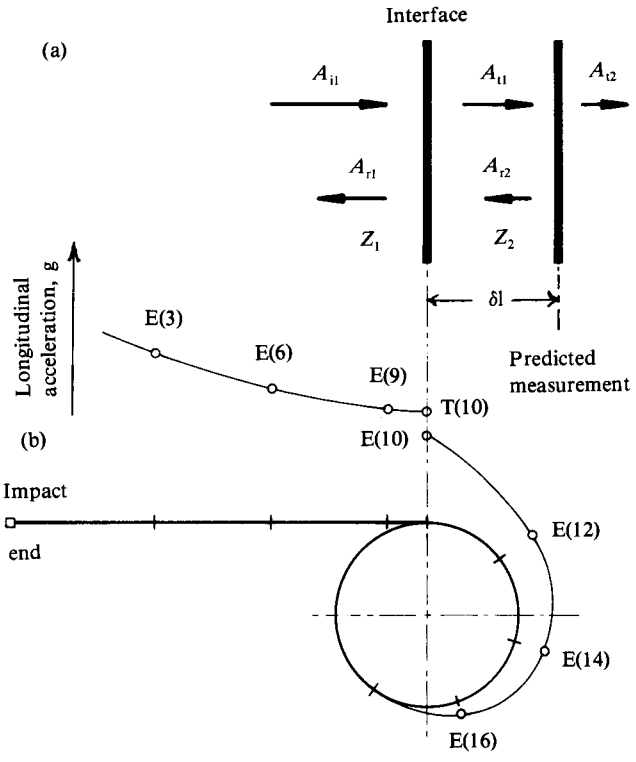

Fig. 3—(a) Wave behaviour in differential element of cable at drum tangent
(b) Experimental acceleration profile of free cable and second layer of cable on drum

Table I gives the results for this series of tests. E(n) represents the experimentally obained maximum acceleration in units of g at station n: thus, for example, for a tension of 140,3 kN, station 6 responded with a maximum acceleration E(6) of 15,81 g, 19,28 g, and 22,00 g for impact masses of 24 kg, 29 kg, and 37 kg respectively.

The general expression for a spatially attentuated wave[3,4] is given by

$$f(x,t) = f_o e^{-\alpha x} e^{i(\omega t - kx)}. \quad \text{.....(1)}$$

For frequency and time independence, the above expression can be simplified to

$$f(x) = f_o e^{-\alpha x}, \quad \text{.....(2)}$$

where f_o is the acceleration in g units at some reference point along the cable. In this investigation, the experimentally determined value of E(3) is used as the reference value f_o above. From Table I, for fixed values of tension, α_{fit} was obtained by the averaging of the attenuation coefficients calculated for each impact mass. For example, for 87,7 kN

$$\alpha_{fit} = \frac{\sum_{i=m_1}^{m_3} \frac{1}{6}\frac{E(9)}{E(3)}}{3} = 0{,}026 \text{ per metre}, \quad \text{.....(3)}$$

TABLE I
EXPERIMENTAL RESULTS

Tension kN	Experimental acceleration, g			α_{fit} m^{-1}	Worst percentage error $\frac{T(n) - E(n)}{E(n)} \times 100$	Impact mass, kg	Experimental acceleration, g			
	E(3)	E(6)	E(9)				E(10)	E(12)	E(14)	E(16)
87,7	16,77	15,46	14,41	0,026	−2,6	24	11,27	5,21	0,97	–
	20,00	18,74	17,03		−1,7	29	14,13	7,22	1,52	–
	23,67	21,85	20,22		−2,0	37	16,79	10,36	2,39	0,50
105,3	17,24	16,10	14,94	0,024	−0,5	24	11,42	4,85	1,12	–
	20,79	19,28	17,88		+0,3	29	14,50	6,88	1,12	–
	24,14	22,37	20,83		−0,1	37	17,24	9,67	2,93	0,44
122,8	16,57	15,64	14,72	0,021	−0,9	24	11,34	4,29	1,09	–
	20,27	19,26	17,85		−1,2	29	14,43	5,62	1,50	–
	23,72	22,10	20,86		+0,7	37	16,37	8,65	2,09	0,49
140,3	16,52	15,81	14,87	0,017	−1,1	24	11,39	4,61	0,73	–
	20,10	19,28	18,25		−1,5	29	14,23	6,16	1,48	–
	23,43	22,00	20,99		+0,7	37	16,65	9,15	2,34	0,66
157,9	16,47	15,61	14,94	0,019	+0,4	24	11,24	3,89	1,05	–
	20,17	19,16	17,88		+2,2	29	14,13	5,40	1,43	–
	23,57	21,82	20,81		+2,8	37	16,62	8,21	2,93	0,40
175,4	16,61	16,03	15,44	0,015	−1,6	24	11,39	4,46	0,86	–
	20,17	19,63	18,32		−1,7	29	14,30	5,75	2,15	–
	23,30	22,54	21,21		−1,1	37	16,79	8,95	3,67	0,69
						24	11,35	4,56	0,98	–
					Average	29	14,28	6,17	1,56	–
						37	16,74	9,16	2,73	0,53

where m_1 = 24 kg, m_2 = 29 kg, and m_3 = 37 kg. Examination of the α_{fit} column of Table I shows a definite trend: as the tension increases, the attenuation coefficients decrease. Furthermore, the magnitude of the impact mass does not appear to affect the attenuation coefficient, i.e. spatial attenuation is independent of the magnitude of the initial stress wave set up in the free cable. This suggests a tension-dependent form of Equation (2) rewritten as

$$f(x,T) = f_o e^{-(\beta/T)x}, \quad \ldots\ldots\ldots\ldots\ldots\ldots\ldots\ldots\ldots\ldots (4)$$

where β is some constant yet to be determined. When $\alpha_{fit} = \beta/T$, the average β is determined by

$$\beta = \frac{\sum_{k=1}^{6} \alpha_{fit}(k)T(k)}{6} = 2566 \text{ m}^{-1}\cdot\text{N}^{-1}. \quad \ldots\ldots (5)$$

Equation (4) then takes the form

$$f(x,T) = f_o e^{-(2566)x/T} = f_o e^{-(1,825 \times 10^{-3})x/\bar{T}}, \quad \ldots\ldots (6)$$

where

$$\bar{T} = T/T_{\text{Breaking load}}.$$

If $T(n) = f(x,T)$ represents the theoretical value obtained above, Table I shows the worst percentage error between the theoretical and the experimental values for each impact mass and tension setting.

Vibration of the Cable on the Drum

Here the increment of the acceleration probe is set to 2 m along the second layer of cable on the drum. As indicated by Fig. 3(b), E(10) is the acceleration experimentally obtained at the drum tangent, E(12) being measured 2 m from E(10), etc.

The determination of the attenuation coefficient for the cable on the drum initially followed the method used for the analysis of the vibration of the free cable. However, errors as high as 400 per cent were common during this exercise, and an alternative approach was therefore pursued. Factors that eventually led to the implementation of a quadratic fit for the acceleration profile along the second layer of cable are based on the following observations taken from Table I.

(1) The depth of penetration of a kinetic shock varies with the magnitude of the acceleration occurring at the interface, i.e. E(10).

(2) It is not apparent, over the limited range of free-cable tension, that the tension affects the degree of penetration around the drum.
(3) The acceleration profile approaches the zero value at definite points along the second layer.

The tension-independence of the function governing the penetration made it possible for the acceleration signals for a given impact mass to be averaged. The result is shown in the bottom part of Table I, where, for example an impact mass of 29 kg, the average experimental acceleration at E(12) is 6,17 g. The following is a more appropriate interpretation of these average values: for an acceleration of 14,28 g at the interface, the pulse will attenuate to 6,17 g at 2 m from the interface, and then to a level of 1,56 g measured 4 m from the interface.

In Fig. 4 the averaged acceleration occurring at the interface is plotted along the ordinate axis as initial conditions. With the curve for an impact mass of 37 kg as a reference, the following procedure was carried out.

(a) The horizontal displacement between each set of curves was found to be a constant for all accelerations.
(b) The data were re-plotted with the horizontal offset, the curvature and magnitude of the shifted curves being preserved in this process.
(c) A least-squares fit of order two was carried out on the combined data (two sets shifted) and the errors were calculated.

This procedure highlighted the fact that the *attenuation* function could be shown to be independent of initial acceleration, and it also provided more data points for the calculation of the least-squares fit.

The errors that were calculated substantiated the fact that penetration is independent of tension and a function of the initial acceleration at the interface.

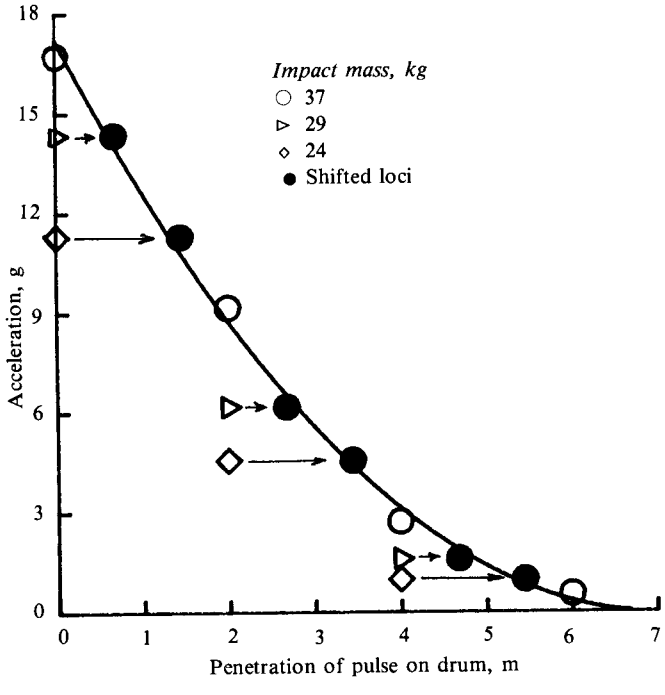

Fig. 4—Space-time-acceleration surfaces generated for different low-pass filter settings

The least-squares fit procedure resulted in the quadratic form

$$H(x)t = 17{,}224 - 4{,}93x + 0{,}352x^2 \text{ g.} \quad \ldots\ldots\ldots (7)$$

The zero of $H(x)$ occurs at

$$H(4{,}93/2(0{,}352)) = 7{,}0 \text{ m.} \quad \ldots\ldots\ldots (8)$$

For a known value of accleration f_o g occurring at the drum–cable interface, the depth of penetration $P(x,f_o)$ is then determined by

$$P(x,f_o) = 7 - [\text{zero of } G(x,f_o)], \quad \ldots\ldots\ldots (9)$$

where

$$G(x,f_o) = (17{,}224 - f_o) - 4{,}93x + 0{,}352x^2. \quad \ldots (10)$$

By use of Equation (9), $P(x,f_o)$ is reduced to a relation solely dependent on f_o:

$$P(f_o) = 1{,}685\ (f_o)^{\frac{1}{2}} \text{ m.} \quad \ldots\ldots\ldots (11)$$

Power Transmission—Free Cable to Drum

The equation for the relationship between the incident, reflected, and transmitted wave at an interface is given by

$$A_r = \left[\frac{1 - Z_2/Z_1}{1 + Z_2/Z_1}\right] A_i$$

$$A_t = \left[\frac{Z_2}{1 + Z_2/Z_1}\right] A_i \quad \ldots\ldots\ldots (12)$$

where an interface can be defined as a plane perpendicular to the direction of propagation of the incident wave, and where the mechanical line impedances Z_n on either side of the plane have different values. The existence of an interface at the drum tangent is due to two factors: the displacement of the cable from a straight line to a circular path, and the friction between the first and the second layer of cable. When the ratio of cable diameter to drum diameter is taken into consideration, the cable deflection (and therefore the friction) at a very small distance past the tangent point is negligible, and thus the mechanical line impedance at that point is almost the same as the value for the free cable. This means that, instead of there being a single well-defined interface at the drum tangent, there is a diffused interface spread over a short distance about the drum tangent point. For the purpose of analysis, this diffused interface can be regarded as a number of incremental interfaces, two of which are shown in Fig. 3(a).

If the secondary reflections are ignored, the total reflected signal will be $A_{r1} + A_{r2}$ separated in time by some interval $\delta l/C$, as shown in Fig. 3(1). For the general case where the diffused interface is approximated by N

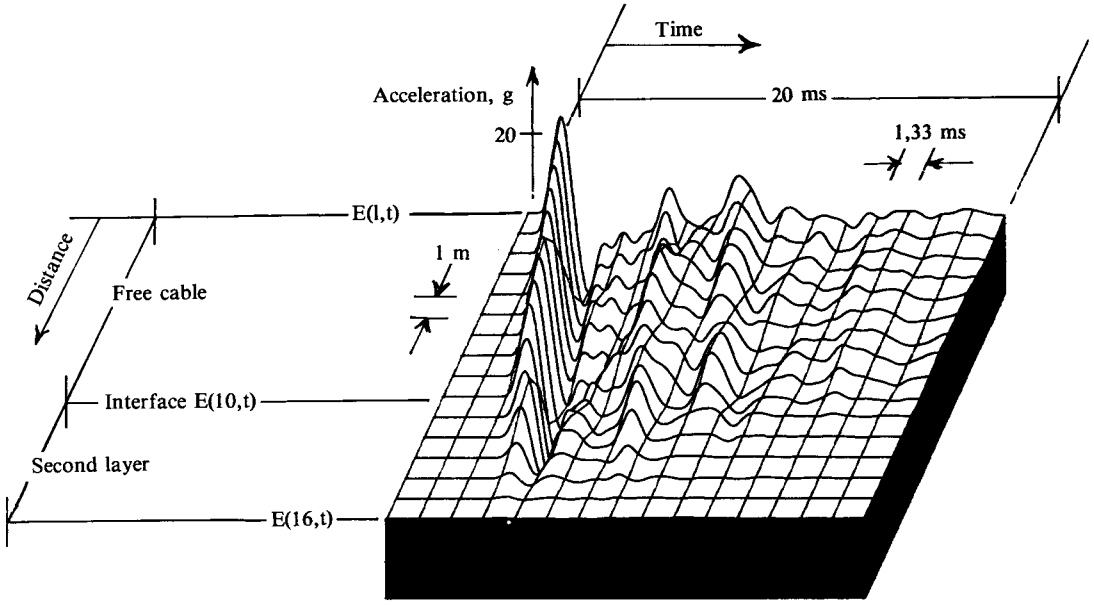

Low-pass filter setting 600 Hz

incremental interfaces spread over a small distance δl, the total reflected signal is given by the summation

$$A_r = \sum_{n=1}^{N} A_{rn}(n\delta t - t), \quad \ldots\ldots\ldots\ldots\ldots\ldots\ldots\ldots (13)$$

where δt is the time difference between the reflected signals. The waveshape of the resulting reflected signal will be a pulse of very low amplitude and long duration compared with the incident pulse (the energy being determined by the area under the curve).

For the detection of such a signal from within a complex waveform, such factors as transducer resonance effects, transducer mounting vibrational effects, and noise had first to be removed from the complex waveform. This was accomplished by low-pass filtering of the detected signals, and the results of this are shown in Fig. 5 for three values of cut-off frequency. This filtering experiment highlighted two facts: firstly, that there were no *discernible* reflected signals owing to the diffusing effect of the drum on the reflected wave as indicated by Equation (13), and secondly that filtering did not corrupt the relative information contained in the first peak of each waveform. This meant that, in the collection of data, low-pass filtering was not necessary. All the experimental data tabulated in Table I were therefore obtained without filtering of the signal from the accelerometer.

With reference to Fig. 3(b), two values are shown at the drum tangent (station 10) for the longitudinal acceleration: T(10), the extrapolated value using the free-cable equation, Equation (6), and E(10), the measured value. The difference in value between T(10) and E(10) is proportional to the amount of energy that is reflected at the diffused interface, but it would be more correct to describe it as being proportional to the maximum value of energy that could be reflected from the interface, since Equation (4) is based on the assumption that the acceleration is continuous in close proximity to the interface.

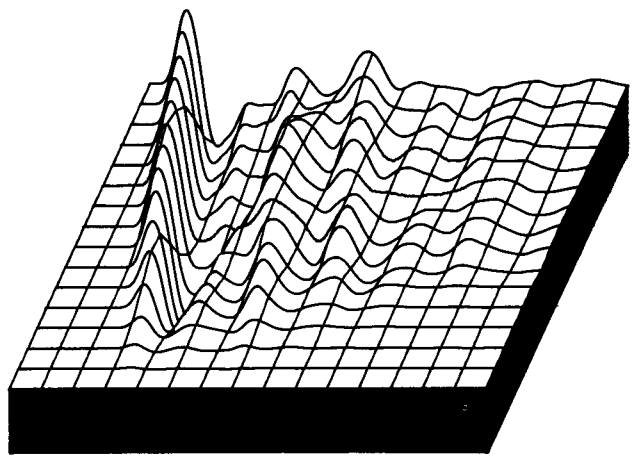

500 Hz

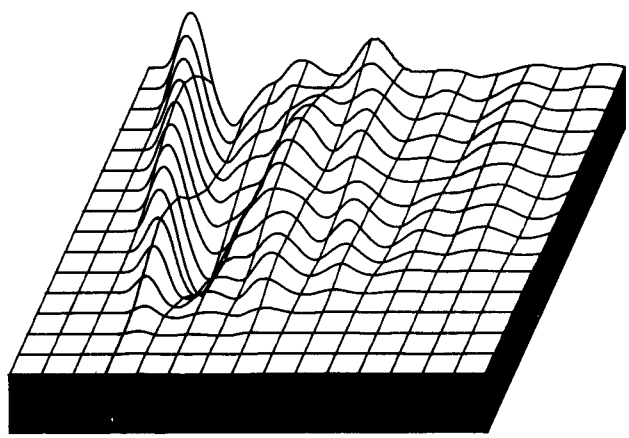

400 Hz

Fig. 5—Least-squares fit (order two) of laterally shifted points

While it is expected that the difference will be very small, this phenomenon is beyond the intended scope of the present work and was not investigated.

The difference between the expected or theoretical value at station 10 using Equation (6), i.e. T(10), and the actual measured value E(10), given by

$$\frac{T(10) - E(10)}{T(10)}, \quad \ldots\ldots (14)$$

gives a measure of the maximum reflection coefficient that can be expected. A mathematical tabulation of Equation (14) based on the information of Table I showed a definite trend: the reflection coefficient increases with increasing tension. However, over the range of impact masses, no definite trend was noticed, i.e. the reflection coefficient appears to be independent of the acceleration.

As power is proportional to $[R(n)\omega]^2$, an expression for the maximum power-transmission coefficient follows directly from Equation (14) and takes the form

$$\left[\frac{E(10)}{T(10)}\right]^2 \quad \ldots\ldots (15)$$

A plot of the maximum reflection and power-transmission coefficients described by Equations (14) and (15) respectively is shown in Fig. 6. Extrapolated values of these coefficients for low tensions or tensions approaching zero indicate that all the power is absorbed by the drum without the creation of any reflected wave. Conversely, for very high tensions, the conditions at the interface approached a rigid or fixed boundary, with the result that incident stress waves are reflected with a corresponding loss of power transmission.

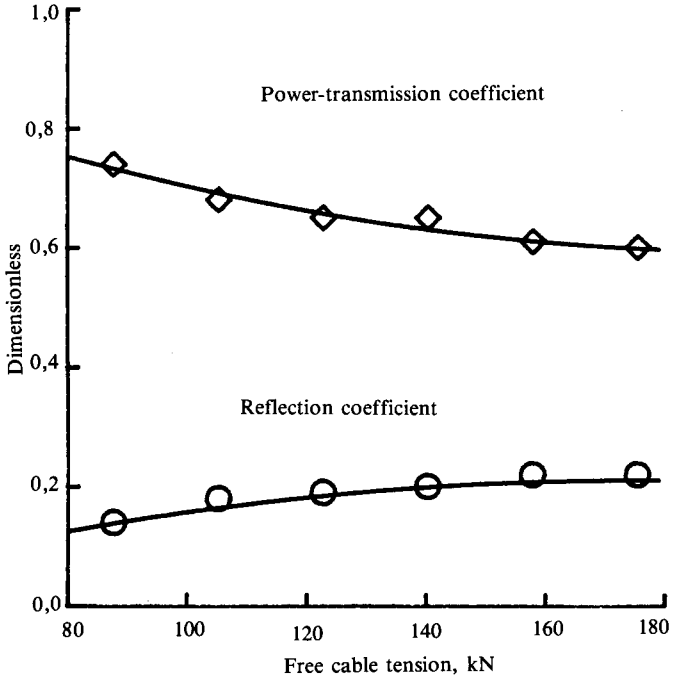

Fig. 6—Least-squares fit (order two) of reflection and transmission coefficients

Discussion of Results

Experimental evidence in the literature on the longitudinal wave properties associated with mine hoisting cables is at best very limited. The pioneering work of Harvey[5] in this field is without doubt the most relevant to the present investigation. Over twenty years ago, he wrote:

> Tests show that in a typical case, the amplitude of a travelling disturbance is attenuated 0,65 percent per 1000 metres of cable and by 1,0 percent at each pair of reflections at the drum and at the conveyance combined.

It is not clear what type of experimental method was used to arrive at the above conclusions. The absence of comment on tension-dependent attenuation and reflection coefficients suggests that the investigator was limited to a single typical tension and shock input (simulated trip-out), an analysis of the envelope of the subsequent decaying acceleration of the conveyance perhaps then being used to quantify the losses and reflection coefficient. A tantalizing question arises here: Would the same purported magnitudes of loss and reflection coefficients be derived for a test in which the mass of the conveyance were reduced to, say, one half of its original value? Experimental evidence in the present investigation indicates that, when a typical tension is halved, the amplitude of a disturbance travelling over 1000 m is reduced by a factor 4×10^{-7}.

Over the range of typical loads for both an empty and a fully loaded skip, the experimentally determined reflection coefficients vary from 0,14 to 0,22 at the winding drum. This is tantamount to approximately 18 per cent of the amplitude of an incident longitudinal disturbance being reflected at the drum–cable interface. In terms of power transmission, this corresponds to 67 per cent of the power being absorbed by the drum. In contrast, Harvey found that over 99 per cent of the incident amplitude is reflected, with a corresponding power loss of 2 per cent upon reflection at the drum.

The penetration of a stress wave round the second layer of cable was found to be a function of the particle acceleration occurring at the interface. An immediate application of this relation, Equation (10), is a determination of the penetration of a pulse resulting from the longitudinal acceleration of the cable as it passes through the cross-over area on a drum fitted with a Lebus liner 180–180°. The largest longitudinal component of acceleration in the cross-over area occurs when, say on the fourth layer, bunching of the cable in the underlying layers causes the tangential velocity to be momentarily accelerated to ± 2 g. A calculation based on Equation (10) shows the penetration in this case to be 2,4 m. Thus, as the cable passes through the cross-over, two stress waves are generated: one propagating up the cable in the direction of the headsheave, and the other penetrating the coil of cable and dissipating itself within 3 m.

For the stress wave leaving the winding drum, another observation is noteworthy: with a cable load of 10 per cent of the breaking load, i.e. 140,6 kN, this stress wave will be attenuated to half its original value within a length of 38 m. Should the cable load be increased to 20 per cent of its breaking load, a 50 per cent reduction in the amplitude will be obtained within a length of 76 m.

It is known that the speed of propagation of a

longitudinal pulse generally increases with increasing tension. In an earlier investigation[6], it was postulated, and successfully observed, that the speed increases rapidly during the initial stages of loading and eventually reaches a plateau before increasing again until the failure load is reached. As these investigators point out, this behaviour is to be expected: as the tension is increased, the cable approaches the geometry of a solid bar due to a gradual tightening of the wires and strands.

Fig. 7 shows the variation in the speed of propagation of a longitudinal pulse as the tension is increased. The speeds are calculated from the arrival and passing times of a pulse (peak-to-peak acceleration) travelling between stations 3 and 6, Fig. 3(b). Attempts to determine if the magnitude of the impact mass influenced the speed of propagation proved unsuccessful between these parameters. Lastly, it can be seen that, over the typical working tensions on a mine, the speed of propagation does not vary by more than 6 per cent.

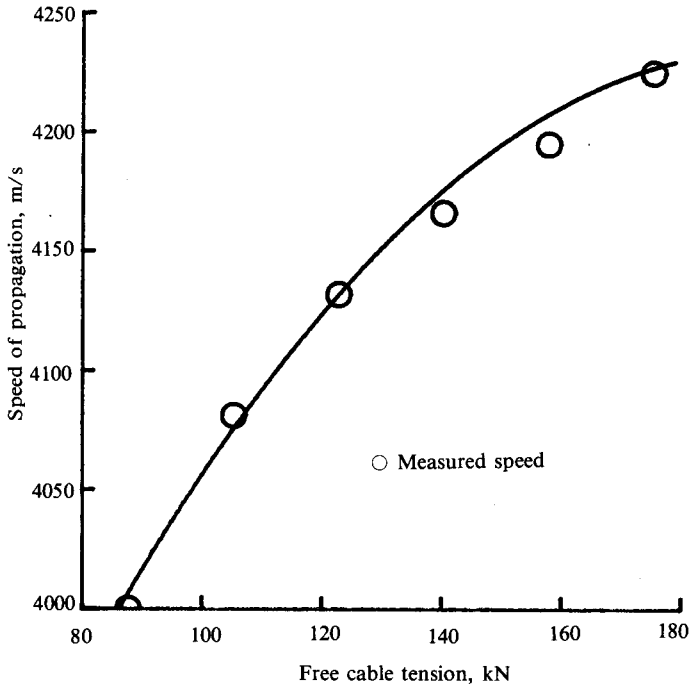

Fig. 7—Least-squares fit (order two) of speed versus tension

A comparison of the research results outlined in this section shows some surprising differences in the quantitative aspects of the findings. An explanation of the apparent divergence of the results will no doubt be forthcoming in future investigations in this field. Perhaps a more sophisticated, controlled experiment would add to the present findings. Alternatively, the implementation of a more formalized mathematical approach and model may offer a better understanding of this under-researched field.

Conclusions

It should be emphasized that the following conclusions are based on the testing of the dynamic response of a single hoisting cable and winding-drum section of fixed geometry. As a result, there may be some difficulties in the application of the following observations to other hoisting cables having different geometries, elastic properties, and environmental installation. However, in spite of these potential differences, certain qualitative trends can be generalized and summarized as follows.

Free Cable under Tension

(1) The longitudinal attenuation coefficient is tension-dependent. For a length of cable free from boundary interferences, the attenuation coefficient decreases with increasing tension. The mathematical form governing the losses associated with a travelling stress wave as experimentally determined is given by

$$f(x) = f_o e^{-(2566)x/T} \text{ (g units)}.$$

(2) The longitudinal attenuation coefficient is independent of the intensity of the travelling stress wave.

Cable Wrapped on Winding Drum (Second Layer and Higher)

(3) The depth of penetration of incident stress waves onto the coil of cable on the winding drum increases with increasing particle acceleration of the wave. Experimental evidence shows the depth of penetration to be governed by the relationship

$$P(f_o) = 1{,}685(f_o)^{1/2} \text{ m},$$

where f_o is the acceleration of the cable at the drum tangent.

(4) Over the limited range of experimental static tensions used, there is no conclusive evidence to suggest that penetration is a function of tension. However, it is postulated that, for low tension (far below the normal tensions of working cables), the penetration will be tension-dependent.

(5) For typical hoisting loads, a maximum of 75 per cent of the energy associated with an incident longitudinal pulse is absorbed by the layers of cable on the winding drum.

(6) The amplitude and width of an incident pulse are decreased and increased respectively after reflection at the cable–drum interface. This is attributed to diffusion of the transmitted and reflected waves in the penetration area arising from infinitesimal changes of mechanical line impedance along the drum tangent.

List of Symbols

a	Effective cross-sectional area of cable (mm^2)
A_i	Amplitude of incident wave
A_r	Amplitude of reflected wave
A_t	Amplitude of transmitted wave
C	Longitudinal wave velocity ($m \cdot s^{-1}$)
E	Young's modulus ($N \cdot mm^{-2}$)
g	Gravitational constant 9,81 ($m \cdot s^{-2}$)
k	Wave number ($2\pi \cdot \lambda^{-1}$)
L	Length (m)
t	Time (s)
T	Longitudinal tension (N)
Z_1	$\rho_1 C_1$ = mechanical line impedance of conducting medium 1 (longitudinal) ($kg \cdot s^{-1}$)

α Spatial attenuation coefficient (m^{-1})
λ Wavelength (m)
ρ Linear mass density of cable ($kg \cdot m^{-1}$)
ω Angular frequency ($rad \cdot s^{-1}$)

Acknowledgements

The authors express their gratitude to Dr Johann Fritz, Head of the Mine Equipment Research Unit of the C S I R, for his enthusiastic support of this project. They thank Mr M. Maduramuthu for the high standards set in the design and commissioning of the laboratory model. Messrs D. Byrne and B. Marcus, with their inimitable technical expertise and advice, made the construction of the model a safe and pleasant task, and Mr D. Singh's keen interest and talent in assisting with the data capture were invaluable. The authors are also indebted to Haggie Rand and Dorbyl Engineering Durban for the generous donations of cable and steel sheeting that made this project possible.

References

1. DIMITRIOU, C., and WHILLIER, A. Vibrations in winding ropes: an appraisal. Johannesburg, Chamber of Mines of South Africa, Project 105/71, Sep. 1973.
2. JORDAN, D.W. A literature survey and recommendations relating to vibrations of wire rope hoists in mines. Johannesburg, Chamber of Mines of South Africa, Project 105/71. 1971.
3. KOLSKY, H. Stress waves in solids. New York, Dover Publications, 1963. pp. 99–129.
4. LINDSAY, R.B. Mechanical radiation. New York, McGraw-Hill, 1960. pp. 74–86.
5. HARVEY, T. 'Escort'—a winder braking system. *J. S. Afr. Inst. Elec. Engrs*, vol. 56, pt 2. 1965. pp. 37–57.
6. VANDERVELDT, H.H., and GILHEANY, J.J. Propagation of a longitudinal pulse in wire ropes under axial loads. *Exp. Mech.*, vol. 13. Oct. 1973. pp. 401–407.

Explosion research

Over the next two years, facilities for research into explosives and coal-dust explosion are to be built at Kloppersbos, 40 km north of Pretoria. The establishment of these facilities is a collaborative effort between the CSIR's National Institute for Coal Research (NICR), the South African Bureau of Standards (SABS), and the Department of Mineral and Energy Affairs.

The explosion tunnels will be used mainly for two purposes. In the first, NICR will study the explosive properties of coal dusts from various South African mines and assist in developing explosion-prevention and safety measures. In the second, the SABS will endeavour to ensure that explosives adhere to set specifications and safety standards.

The new coal-dust explosion tunnel will be known as the G.P. Badenhorst Test Gallery in honour of the Government Mining Engineer, who has striven for many years to obtain such a facility and generally to improve safety in mining.

The test facilities are to be inaugurated in 1987.

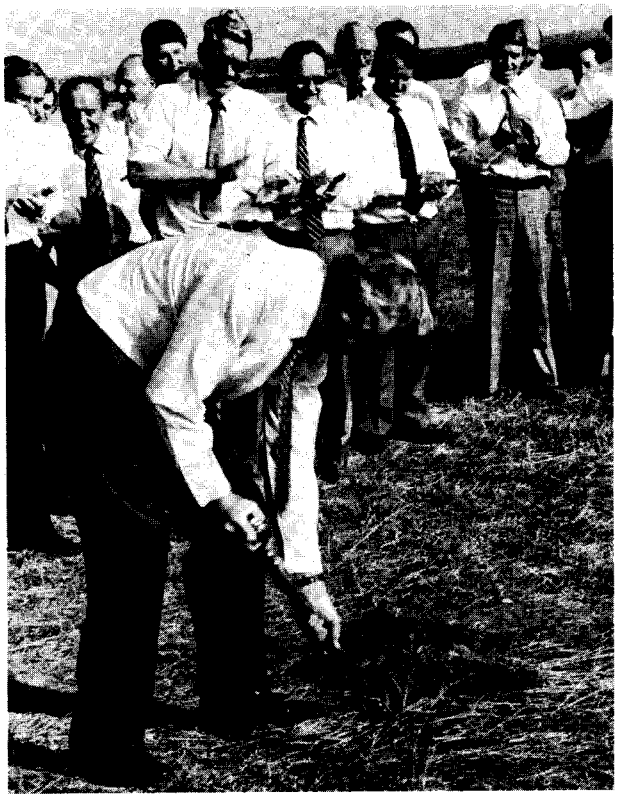

Mr D.W. Steyn, Minister of Mineral and Energy Affairs, turning the first sod for the test facilities at Kloppersbos